Models for Copper-Containing Proteins: Structure and Properties of Novel Five-Coordinate Copper(I) Complexes

Robert R. Gagné,* Judith L. Allison, Robert S. Gall, and Carl A. Koval

Contribution No. 5554 from the Division of Chemistry and Chemical Engineering, California Institute of Technology, Pasadena, California 91125. *Received March 31, 1977*

Abstract: The four-coordinate Cu(I) complex [difluoro-3,3′-(trimethylenedinitrilo)bis(2-butanone oximato)borate]copper(I), $Cu(LBF_2)$, can be produced by electrochemical reduction of the corresponding Cu(II) complex. The Cu(I) complex reacts with monodentate ligands (e.g., CO, 1-methylimidazole, acetonitrile) yielding five-coordinate adducts. The structure of the carbonyl derivative has a square-pyramidal copper displaced 0.96 Å out of the basal nitrogen plane. The Cu–CO distance is 1.780 (3) Å, with a Cu–C–O angle of 177.5 (3)°. The C–O bond length is 1.112 (4) Å. The space group is *Pbca* with a = 13.926 (1) Å, b = 14.209 (1) Å, c = 16.297 (1) Å, Z = 8, and R = 5.5%. Preliminary equilibrium constants were determined by cyclic voltammetry and by absorption spectroscopy. Carbon monoxide ($K_c = 4.7 \times 10^4\ M^{-1}$) binds significantly better than 1-MeIm ($K_c = 16\ m^{-1}$). The possible biochemical significance of five-coordinate Cu(I) is discussed.

Introduction

Numerous copper-containing proteins utilize molecular oxygen in respiratory and biosynthetic functions.[1-3] The best studied copper proteins, hemocyanin and tyrosinase, serve, respectively, in O_2 transport and in activating O_2 for the oxidation of tyrosine.[4] Both tyrosinase and hemocyanin apparently contain a pair of contiguous Cu atoms, commonly designated type III copper, at the active site. The structural nature of the type III copper site is not known for any protein. Stoichiometry,[13,14] EPR,[15-19] and magnetic susceptibility measurements[18-20] on various derivatives of hemocyanin and tyrosinase, however, suggest a strongly antiferromagnetically coupled pair of copper atoms separated by some 3–5 Å.[5-7] The number and identity of ligands bound to either copper are not known. Nonetheless, titration[21,22] and spectroscopic[23,24] studies tend to preclude sulfur and favor nitrogen ligands, probably imidazole nitrogen.

The paucity of structural and mechanistic information for these copper proteins is paralleled by an equally sparse literature on the reactions of Cu(I) complexes, particularly with nitrogen ligands.[25] Extreme lability, facile disproportionation, and air sensitivity have frustrated attempts to explore reactions of copper–nitrogen ligand complexes. For example, there are no well-characterized dioxygen complexes derived from Cu(I)[26] despite the large number of O_2 complexes known for several other metals.[27-30]

To help elucidate possible active site structures and mechanisms of copper protein activity, we are exploring the basic relationships between structure and chemical reactivity in a variety of Cu(I) complexes of predominantly nitrogen ligands. Both mononuclear and binuclear complexes are under investigation, in the hopes of eventually explaining the apparent necessity for a binuclear copper site (type III) for O_2 binding in the proteins.[4] Herein we report the synthesis and properties of novel *five*-coordinate Cu(I) complexes which have been communicated previously.[31]

Results and Discussion

Deducing structure–reactivity relationships for Cu(II) complexes is complicated by a number of factors which can be controlled, as follows.

(1) Both Cu(I) and Cu(II) are rather substitution labile.[25-33] Thus, complexes of monodentate and even bidentate ligands often lead to solutions containing several species including two-, three- and four-coordinate monomers as well as dimers, etc. Use of polydentate ligands, including macrocycles, inhibits both dissociation and dimer formation (via bridging atoms of the polydentate ligand) especially if the chelate is somewhat rigid structurally, as macrocycles are. Explaining solution behavior, especially in reference to solid-state structures, is thus simplified appreciably.

(2) Many Cu(I) complexes disproportionate rapidly at the ambient temperature to Cu(II) and Cu(0).[33] Ligand environments having saturated amines and/or an enforced rigid, square-planar structure destabilize Cu(I) with respect to Cu(II), as shown by electrochemical studies.[34,35] Conversely, employing flexible yet unsaturated nitrogen ligands should preclude disproportionation.

(3) Reducing Cu(II) to Cu(I) without undesirable further reduction to Cu(0) is difficult with most common chemical reducing agents. Likewise, complexing Cu(I) directly by reaction between some appropriate Cu(I) salt and a polydentate ligand most often leads to disproportionation, possibly owing to unstable intermediates.[36-39] Electrochemical reduction at constant potential has, however, been shown[35] to be both specific and practical.

(4) Finally, it must be recognized that most Cu(I) complexes are very air-sensitive. Schlenk, vacuum-line, and modern inert-atmosphere chamber techniques render this a relatively trivial problem.

After examining several other polydentate and macrocyclic ligand systems, the results of which are reported in part elsewhere,[39] we have found the tetradentate ligand **1** to adequately fulfill the requirements above and to yield novel Cu(I) chemistry.[31] The free ligand, 3,3′-(trimethylenedinitrilo)bis(2-butanone dioxime) (**1**, H_2L), has been prepared previously,[40] using boiling diisopropyl ether as solvent, although this procedure is difficult. Large quantities of ligand can be obtained far more simply, however, by combining 2,3-butanedione monoxime with 1,3-diaminopropane in ethanol at 25 °C (eq 1).

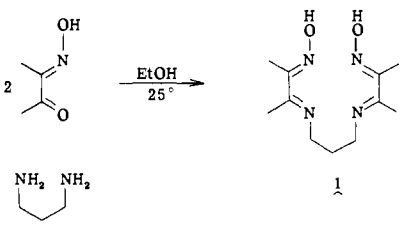

(1)

1

Treating warm acetone or ethanol solutions of the macrocycle **1** with Cu(II) salts gives red to green mixtures depending on the ligand to Cu(II) ratio. With a twofold excess of ligand,

Table I. Cyclic Voltammetric Data for $[Cu(LBF_2)ClO_4]_2 \cdot C_4H_8O_2$ (5)[a]

Solvent	E_{pc},[b] V	E_{pa},[b] V	E^f,[b,c] V	i_{pc}, μA	i_{pa}, μA
CH_3CN	−0.432	−0.330	−0.381	18	19
$(CH_3)_2CO$	−0.459	−0.345	−0.402	18	17

[a] Conditions: [Cu] = 2×10^{-3} M under inert atmosphere; sweep rate = 100 mV/s; hanging mercury drop electrode. [b] Potentials are given vs. SHE as calculated in Table X. [c] $E^f = (E_{pc} + E_{pa})/2$.

dark red-brown, crystalline $Cu(HL)ClO_4 \cdot H_2O$ (2) can be isolated. The product is contaminated with excess copper, possibly because of small amounts of a binuclear species such as 3. This species may be similar to the Cu(II) complex obtained[41] with salicylaldehydeethylenediamine, 4.

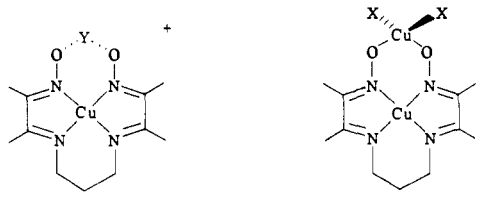

2, Y = H
5, Y = BF_2

3

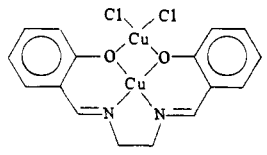

4

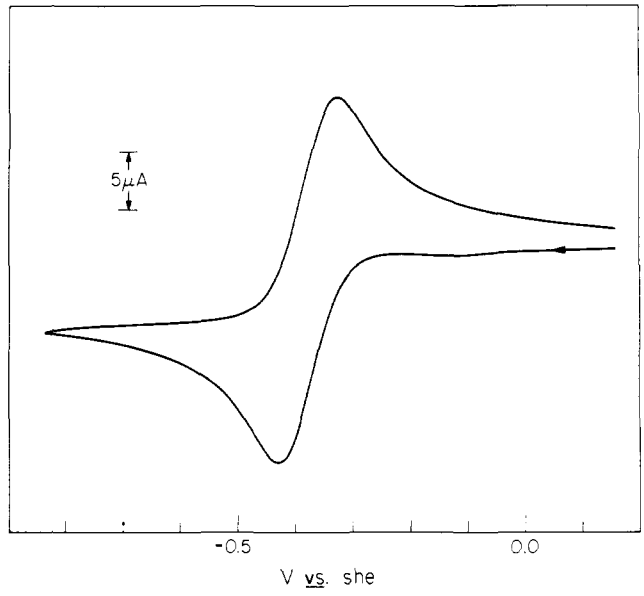

Figure 1. Cyclic voltammetry of $[Cu(LBF_2)(ClO_4)]_2 \cdot C_4H_8O_2$ (5) in CH_3CN. Scan rate = 100 mV/s. [Cu] = 2×10^{-3} M.

To inhibit binding of a second copper atom and to prevent possible hydrogen atom transfer reactions (as to dioxygen coordinated to copper), the bridging oxime hydrogen in 2 was replaced with BF_2 via treatment with boron trifluoride etherate in dioxane. The resulting complex has an analysis consistent with the formulation $[Cu(LBF_2)ClO_4]_2 \cdot C_4H_8O_2$ (5). It has not been determined whether dioxane is acting as a μ-bidentate bridge between two coppers or is present simply as solvent of crystallization.

The reduction of complex 5 was attempted by several chemical reducing agents, including Na, Zn, Mg, and their amalgams, and hydrazine. In all cases some Cu(0) was produced, by direct reduction of Cu(II) or by disproportionation of intermediate Cu(I) species. For this reason, the electrochemical behavior of the complex was examined.

Cyclic voltammograms of 5 have been obtained both in acetonitrile and in acetone. A scan, representative of the first reduction process in either solvent, is given in Figure 1.[42] While the anodic and cathodic peak currents are nearly equal, the peak potential separation is much larger than the 58 mV expected for a reversible, one-electron process. That this reduction does involve only a single electron is confirmed by constant potential electrolysis at potentials slightly negative of the wave (~ −0.7 V) yielding n values of 1.0 ± 0.05.

The potential of the Cu(II)/Cu(I) couple for 5 (E^f = −0.381; see Table I) is more positive than that for complex 2 (E^f = −0.560; see Experimental Section) indicating a possible stabilization of Cu(I) in the former. Indeed, gram quantities of $Cu(LBF_2)$ (6) can be synthesized by CPE at −0.7 V. During the electrolysis, the original purple solution (Cu(II)) becomes deep blue (Cu(I), λ_{max} 677 nm) with subsequent precipitation of a microcrystalline, red solid. The product, which is blue upon being ground to a powder (an optical phenomenon since there is no other indication of chemical decomposition), is apparently not air-sensitive in the solid state.

In a formal sense the blue Cu(I) complex, $Cu(LBF_2)$, 6, is a four-coordinate 18-electron system and as such is coordinatively saturated. Nonetheless, 6 reacts with a number of monodentate ligands to give presumably five-coordinate Cu(I) complexes. For example, addition of 1-methylimidazole, (1-MeIm) to the blue complex 6 in acetone gives a green solution (λ_{max} 420 nm) from which the imidazole adduct, $Cu(LBF_2)$(1-MeIm) (7) can be isolated. Even acetonitrile, usually considered a weak ligand, binds to $Cu(LBF_2)$ (6), giving aquamarine solutions at 25 °C. Green acetonitrile solutions result upon cooling to −40 °C, presumably indicating a greater degree of complex formation at the lower temperature.

Most surprisingly, carbon monoxide reacts rapidly with blue $Cu(LBF_2)$ (6) solutions at 25 °C, yielding light yellow solutions. The reaction is readily reversed upon purging with nitrogen. A stable carbonyl adduct can be isolated from CO treated solutions as a bright yellow microcrystalline material (ν_{CO} 2068 cm^{-1}), $Cu(LBF_2)(CO)$ (8). The solution infrared spectrum of $Cu(LBF_2)(CO)$ (8), (CH_2Cl_2, 1 atm CO) shows only a single peak attributable to coordinated CO (ν_{CO} 2080 cm^{-1}). This is consistent with the presence of a single carbonyl species in solution. Finally, the similarity between ν_{CO} in solution (2080 cm^{-1}) and in the solid state (2068 cm^{-1}) suggests that the solution species is most probably a five-coordinate, monocarbonyl adduct (vide infra).

Crystal Structure

The carbonyl adduct $Cu(LBF_2)(CO)$ (8) was easily crystallized by evaporation of an acetone solution, permitting a structural determination. Figure 2 shows the structure and labeling scheme of the novel copper(I) carbonyl complex while Table II details the crystal data. The structure's uniqueness lies in five-coordination for copper(I) which gives rise to a 20-electron count for the metal atom coordinated to five two-electron donors. Although five-coordination is known for other d^{10} metals,[43] it is not common for copper(I). In addition,

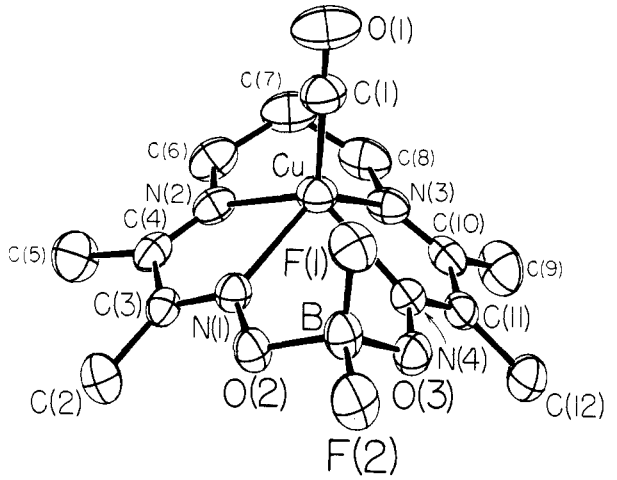

Figure 2. An ORTEP drawing of the structure and numbering scheme of $Cu(LBF_2)(CO)$ (**8**) with thermal ellipsoids at the 40% probability level. Hydrogen atoms are omitted.

Table II. Crystal Data for $Cu(LBF_2)(CO)$ (**8**)

Formula	$Cu(BF_2C_{11}H_{18}N_4O_2)CO$
FW	378.64
Space group	D_{2h}^{15}-*Pbca* (no. 61)
a	13.926 (1) Å
b	14.209 (1) Å
c	16.297 (1) Å
V	3224.8 Å^3
Z	8
ρ_{calcd}	1.56 g cm^{-3}
ρ_{obsd}	1.55 (3) g cm^{-3}
λ(Cu K$\bar{\alpha}$)	1.5418 Å
μ(Cu K$\bar{\alpha}$)	23.293 cm^{-1}

Table III. Bond Distances (Å)

Cu-N1	2.165 (2)	N1-C3	1.275 (3)
Cu-N4	2.163 (2)	N2-C4	1.277 (4)
Cu-N2	2.100 (2)	N2-C6	1.459 (4)
Cu-N3	2.108 (2)	C2-C3	1.488 (4)
		C3-C4	1.485 (4)
Cu-C1	1.780 (3)	C4-C5	1.484 (5)
O1-C1	1.112 (4)	C7-C8	1.500 (5)
F1-B	1.386 (4)		
F2-B	1.379 (4)	C2-H1	0.86 (3)
O3-B	1.478 (4)	C2-H2	0.93 (3)
O2-B	1.475 (4)	C2-H3	0.93 (3)
		C5-H4	0.82 (3)
O2-N1	1.374 (3)	C5-H5	1.05 (3)
O3-N4	1.371 (3)	C5-H6	0.89 (3)
		C6-H7	0.85 (3)
N4-C11	1.283 (3)	C6-H8	1.02 (3)
N3-C10	1.269 (4)	C7-H9	0.92 (3)
N3-C8	1.471 (4)	C7-H10	0.91 (3)
C11-C12	1.480 (4)	C8-H11	1.01 (3)
C10-C11	1.494 (4)	C8-H12	0.97 (3)
C9-C10	1.497 (5)	C9-H13	0.98 (3)
C6-C7	1.502 (5)	C9-H14	0.97 (3)
		C9-H15	0.89 (3)
		C12-H16	0.90 (3)
		C12-H17	0.94 (3)
		C12-18	0.87 (3)

$Cu(LBF_2)(CO)$ (**8**) is one of the few structurally characterized copper(I) carbonyl complexes and is apparently the only known 20-electron complex containing coordinated carbon monoxide.

Tables III and IV give bond lengths and angles for $Cu(LBF_2)(CO)$ (**8**). All nonhydrogen intermolecular separations are greater than 3.39 Å. There is no evidence for intermolecular or intramolecular hydrogen bonding.

Table IV. Bond Angles (Deg)

N2-Cu-N4	124.7 (1)	F1-B-F2	110.7 (3)
N1-Cu-N3	127.6 (1)	F1-B-O2	110.7 (3)
N1-Cu-N4	79.1 (1)	F1-B-O3	110.8 (3)
N2-Cu-N3	85.9 (1)	F2-B-O2	105.1 (3)
N3-Cu-N4	73.8 (1)	F2-B-O3	105.8 (3)
N1-Cu-N2	73.9 (1)	O2-B-O3	113.4 (3)
Cu-N1-O2	126.4 (2)	O3-N4-C11	116.0 (2)
Cu-N4-O3	126.2 (2)	O2-N1-C3	115.7 (2)
Cu-N1-C3	117.5 (2)	N1-O2-B	112.5 (2)
Cu-N2-C4	118.0 (2)	N4-O3-B	112.9 (2)
Cu-N2-C6	120.2 (2)		
Cu-N3-C8	119.4 (2)	N1-C3-C2	123.9 (3)
Cu-N3-C10	118.5 (2)	N1-C3-C4	113.6 (3)
Cu-N4-C11	117.8 (2)	N2-C4-C5	124.3 (3)
		N2-C4-C3	116.3 (3)
N1-Cu-C1	114.9 (1)	N3-C10-C9	125.6 (3)
N2-Cu-C1	114.8 (1)	N3-C8-C7	112.4 (3)
N3-Cu-C1	117.4 (1)	N4-C11-C10	113.3 (3)
N4-Cu-C1	120.3 (1)	N4-C11-C12	124.4 (3)
		C4-N2-C6	121.8 (3)
Cu-C1-O1	177.5 (3)	N2-C6-C7	112.2 (3)
		C8-N3-C10	122.0 (3)
		N_3-C10-C11	116.3 (3)
		C_2-C_3-C_4	122.3 (3)
		C_3-C_4-C5	119.3 (3)
		C9-C10-C11	118.0 (3)
		C10-C11-C12	122.1 (3)
		C6-C7-C8	117.1 (3)

Table V. Root-Mean Square Amplitudes of Vibration along the Principal Axes (Å)

Cu	0.21	0.23	0.24
F1	0.22	0.26	0.28
F2	0.19	0.26	0.34
O1	0.20	0.39	0.40
O2	0.19	0.21	0.27
O3	0.21	0.22	0.26
N1	0.20	0.22	0.23
N2	0.19	0.22	0.27
N3	0.19	0.23	0.27
N4	0.20	0.22	0.23
C1	0.22	0.25	0.28
C2	0.22	0.26	0.29
C3	0.19	0.20	0.24
C4	0.19	0.21	0.27
C5	0.22	0.30	0.35
C6	0.21	0.27	0.32
C7	0.20	0.29	0.34
C8	0.20	0.28	0.34
C9	0.22	0.30	0.35
C10	0.19	0.21	0.29
C11	0.19	0.20	0.27
C12	0.22	0.26	0.32
B	0.20	0.22	0.27

The carbonyl complex $Cu(LBF_2)(CO)$ (**8**) exhibits idealized C_s-*m* geometry with no crystallographically imposed symmetry. The copper atom sits in an asymmetrical square-pyramidal environment and is displaced 0.96 Å from the basal plane of the four nitrogen atoms. Two significantly different sets of Cu-N bond lengths which average 2.164 and 2.104 Å characterize the equatorial asymmetry. The trans N-Cu-N angles are 124.7 (1) and 127.6 (1)°; the cis N-Cu-N angles range from 73.8 (1) to 85.9 (1)°.

The carbonyl ligand coordinates at the apex of the square-pyramid with a Cu-CO distance of 1.780 (3) Å and a Cu-C-O angle of 177.5 (3)°. The C-O bond length, which has not been corrected for possible vibrational shortening (Table V), is 1.112

Table VI. Atomic Coordinates[a] for $Cu(LBF_2)(CO)$ (**8**)

Atom	*X*	*Y*	*Z*	
Cu	23458 (3)	10234 (3)	41603 (3)	
F1	3529 (1)	1537 (1)	5685 (1)	
F2	2753 (1)	1957 (1)	6857 (1)	
O1	4321 (2)	962 (2)	3617 (2)	
O2	2120 (1)	2451 (1)	5651 (1)	
O3	2092 (2)	787 (2)	6083 (1)	
N1	1940 (2)	2274 (2)	4836 (2)	
N2	1434 (2)	1791 (2)	3383 (2)	
N3	1478 (2)	−147 (2)	3874 (2)	
N4	1919 (2)	416 (2)	5321 (2)	
C1	3568 (2)	986 (3)	3843 (2)	
C2	1004 (3)	3726 (2)	4873 (2)	
C3	1408 (2)	2873 (2)	4472 (2)	
C4	1168 (2)	2609 (2)	3614 (2)	
C5	625 (3)	3281 (3)	3094 (2)	
C6	1164 (3)	1411 (3)	2584 (2)	
C7	1554 (3)	437 (3)	2449 (2)	
C8	1206 (3)	−322 (3)	3015 (2)	
C9	586 (3)	−1535 (2)	4363 (3)	
C10	1182 (2)	−664 (2)	4457 (2)	
C11	1425 (2)	−346 (2)	5305 (2)	
C12	1071 (3)	−844 (2)	6043 (2)	
B	2643 (3)	1675 (2)	6053 (2)	
Atom	***X***	***Y***	***Z***	***B***
H1	135 (2)	422 (2)	479 (2)	5.20
H2	99 (2)	365 (2)	544 (2)	5.20
H3	40 (2)	389 (2)	468 (2)	5.20
H4	8 (2)	307 (2)	310 (2)	6.90
H5	79 (2)	325 (2)	246 (2)	6.90
H6	40 (2)	381 (2)	331 (2)	6.90
H7	136 (2)	178 (2)	220 (2)	6.30
H8	43 (2)	140 (2)	262 (2)	6.30
H9	222 (2)	46 (2)	249 (2)	6.80
H10	134 (2)	24 (2)	195 (2)	6.80
H11	50 (2)	−48 (2)	298 (2)	6.60
H12	146 (2)	−94 (2)	290 (2)	6.60
H13	75 (2)	−180 (2)	383 (2)	7.10
H14	82 (2)	−200 (2)	475 (2)	7.10
H15	1 (2)	−144 (2)	458 (2)	7.10
H16	110 (2)	−47 (2)	648 (2)	5.80
H17	40 (2)	−87 (2)	603 (2)	5.80
H18	136 (2)	−137 (2)	614 (2)	5.80

[a] The *X*, *Y*, and *Z* fractional coordinates are multiplied by 10^5 for the copper atom, 10^4 in the case of the nonhydrogen atoms, and by 10^3 otherwise.

(4) Å. To our knowledge the only other copper(I) carbonyl complex which has been structurally characterized is [hydrotris(1-pyrazolyl)borato]copper(I) carbonyl, $[HB(pz)_3]CuCO$.[44] The latter complex has a four-coordinate copper(I) atom with a closed-shell configuration. Carbon monoxide is bonded linearly; the Cu–CO distance averages 1.765 Å and the C–O bond length is 1.120 Å. Thus, while the average Cu–N distance in $Cu(LBF_2)(CO)$ (**8**) is 0.09 Å longer than that in $[(HB(pz)_3)]CuCO$, both the Cu–CO and CO distances agree closely in spite of the difference in coordination numbers of the copper atom. As we have previously noted,[31] the carbonyl infrared stretching frequencies also show only a small variation despite the different coordination geometries for copper(I).

Several structural determinations of various metals coordinated to H_2L (**1**, or its derivatives) have been reported. These include six-coordinate d^6 metals Rh(III)[45a] and Co(III).[45b] A closely related copper(II) complex,[46] which has a saturated Cu–N (amine) bond, is square pyramidal with a perrhenate anion occupying the axial coordination site. The Cu–N bond lengths in $Cu(LBF_2)(CO)$ (**8**) average 0.16 Å longer than

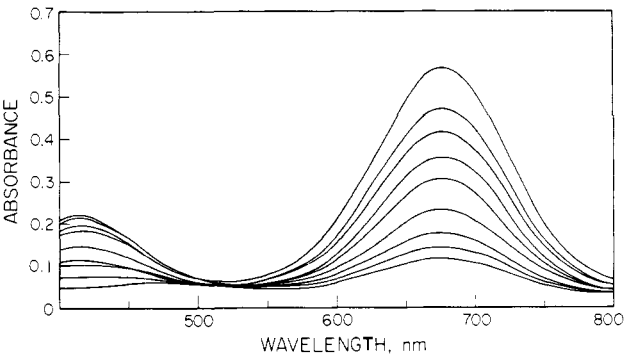

Figure 3. Visible spectral changes observed on addition of 1-methylimidazole to a solution of $Cu(LBF_2)$ (**6**) in acetone.

those in the copper(II)–amine complex. The copper(II) ion is displaced only 0.24 Å out of the plane of the equatorial nitrogen atoms.[46] Presumably, the larger size of the copper(I) ion accounts for the larger displacement of the metal atom from the plane of the four nitrogen atoms in $Cu(LBF_2)(CO)$ (**8**).

Rhodium(I) complexes of H_2L (**1**) have been found to be very reactive toward oxidative addition.[47] In some cases cis addition is indicated which would require distortion of the macrocycle from planarity. The macrocycle is nearly planar in the Rh(III), Rh(I), and Co(III) structures. In $Cu(LBF_2)(CO)$ (**8**), however, the macrocycle deviates considerably from planarity as evidenced by a dihedral angle of 60.0° between the Ni(1)–C(3)–C(4)–N(2) and N(3)–C(10)–C(11)–N(4) planes. This angle is less than 3° for the d^6 and d^8 complexes.

Other differences in the conformation of the macrocycle in the structures of the six-coordinate BF_2-bridged Rh(III) complex, $Rh[C_2(LBF_2)](CH_3)(I)$,[45a] and of $Cu(LBF_2)(CO)$ (**8**) are evident. In the latter complex, atom C(7) and the boron atom both lie above the plane of the four equatorial nitrogen atoms. A "boat" conformation is thus produced for the two six-membered rings which include the metal atom. In the Rh(III) complex, however, these atoms are located on opposite sides of the macrocycle plane leading to an overall "chair" conformation. This variation in conformation presumably results from the difference in steric requirements of both the metal atoms and the axial ligands in the Cu(I) and Rh(III) complexes.

The average values of the C=N, C—N, and C—C bond lengths in $Cu(LBF_2)(CO)$ (**9**) are 1.276 ± 0.006, 1.465 ±

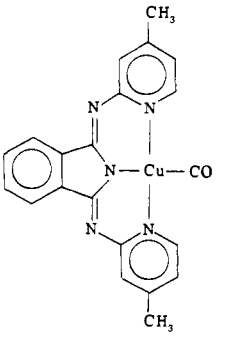

9

0.008, and 1.491 ± 0.008 Å, respectively.[48] For comparison, values of 1.300 ± 0.013, 1.476 ± 0.018, and 1.506 ± 0.025 Å are found for $Rh[C_2(LBF_2)](CH_3)I$.

The refined C–H bond lengths average 0.93 ± 0.06 Å. The H–C–H angles range from 89 to 129° with a mean value of 107 ± 10°.

Tables VI and VII give the atomic coordinates and the anisotropic thermal parameters for $Cu(LBF_2)(CO)$ (**8**).

Table VII. Anisotropic Thermal Parameters for $Cu(LBF_2)(CO)$ (**8**)

Atom	U_{11}	U_{22}	U_{33}	U_{12}	U_{13}	U_{23}
Cu	448 (2)	552 (3)	565 (3)	−10 (2)	59 (2)	−18 (2)
F1	51 (1)	68 (1)	74 (1)	2 (1)	−10 (1)	−2 (1)
F2	96 (2)	70 (1)	49 (1)	12 (1)	−28 (1)	−6 (1)
O1	61 (2)	155 (3)	132 (3)	−8 (2)	41 (2)	1 (2)
O2	64 (1)	45 (1)	43 (1)	7 (1)	−11 (1)	−2 (1)
O3	69 (2)	49 (1)	45 (1)	3 (1)	−3 (1)	3 (1)
N1	50 (2)	46 (2)	42 (2)	1 (1)	−4 (1)	3 (1)
N2	52 (2)	68 (2)	38 (2)	−9 (2)	−2 (1)	2 (1)
N3	54 (2)	53 (2)	57 (2)	−4 (1)	5 (1)	−18 (1)
N4	47 (1)	41 (1)	50 (2)	4 (1)	2 (1)	0 (1)
C1	56 (2)	64 (2)	69 (2)	−4 (2)	13 (2)	−2 (2)
C2	70 (2)	55 (2)	74 (2)	10 (2)	−11 (2)	2 (2)
C3	40 (2)	43 (2)	49 (2)	−4 (1)	−1 (1)	8 (1)
C4	45 (2)	64 (2)	46 (2)	−4 (2)	−1 (2)	16 (2)
C5	94 (3)	99 (3)	66 (2)	27 (2)	−13 (2)	15 (2)
C6	82 (3)	92 (2)	44 (2)	−14 (2)	−4 (2)	1 (2)
C7	84 (3)	108 (3)	48 (2)	−6 (3)	2 (2)	−26 (2)
C8	78 (2)	77 (3)	78 (3)	−8 (2)	3 (2)	−37 (2)
C9	85 (3)	54 (2)	125 (4)	−16 (2)	−6 (3)	−8 (2)
C10	41 (2)	40 (2)	83 (3)	2 (2)	3 (2)	−11 (2)
C11	41 (2)	40 (2)	71 (2)	4 (1)	9 (2)	6 (2)
C12	73 (2)	56 (2)	92 (3)	−1 (2)	16 (2)	15 (2)
B	64 (2)	47 (2)	49 (2)	4 (2)	−14 (2)	0 (2)

[a] The form of the thermal ellipsoid is $\exp[-2\pi^2(U_{11}h^2a^{*2} + \ldots + 2U_{23}klb^*c^*)]$. The U_{ij} elements are multiplied by 10^4 for the copper atom and by 10^3 otherwise.

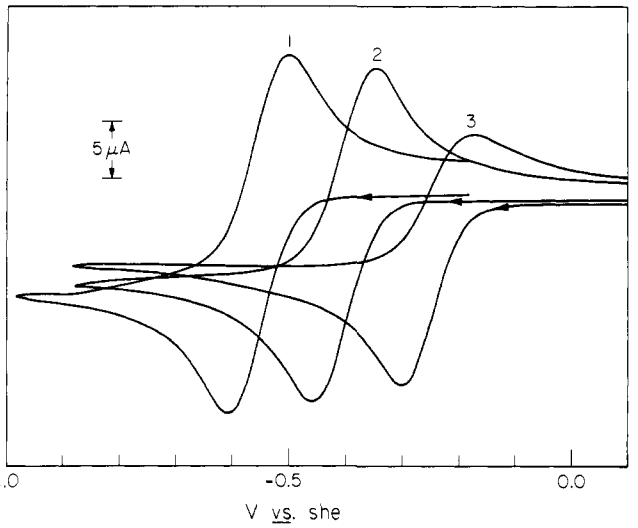

Figure 4. Cyclic voltammetry of $[Cu(LBF_2)(ClO_4)]_2 \cdot C_4H_8O_2$ (**5**) in acetone: (1) with 100 equiv 1-MeIm; (2) under N_2; and (3) with 1 atm CO. Scan rate = 100 mV/s. Concentrations of Cu(II) were not held precisely equal, $\simeq 2 \times 10^{-3}$ M.

Equilibrium Constants. Preliminary equilibrium (concentration) constants for the formation of five-coordinate complexes, $Cu(LBF_2)L'$ (eq 2)

$$Cu(LBF_2) + L' \overset{K_c}{\rightleftharpoons} Cu(LBF_2)L' \qquad (2)$$

have been determined via spectroscopic studies and by monitoring changes in electrochemical redox behavior upon addition of ligands, L', as follows.

The blue four-coordinate Cu(I) complex $Cu(LBF_2)$ (**6**) has a strong absorption at 677 nm (acetone, ϵ 1.03×10^4 M^{-1} cm^{-1}, 25 °C) which disappears upon addition of a large excess of CO or 1-MeIm. Monitoring the absorption at 677 nm as ligand was added was used to determine the extent of formation of the five-coordinate complex (eq 2). Figure 3 depicts the series of spectra obtained upon adding various amounts of

Table VIII. Equilibrium Constants for the Formation of Five-Coordinate Complexes $Cu(LBF_2)L'$ in Acetone

$$Cu(LBF_2) + L' \overset{K}{\rightleftharpoons} Cu(LBF_2)L'$$

L'	K	Method
1-MeIm	$K_c = 16$ M^{-1}	EAS
CO	$K_p = 500$ atm^{-1} ($P_{1/2} = 1.5$ mm)	EAS
CO	$K_c \cong 4.7 \times 10^4$ M^{-1}	EAS
CO	$K_c \cong 6.7 \times 10^4$ M^{-1}	ΔE^f

1-MeIm to an acetone solution of the four-coordinate complex, $Cu(LBF_2)$ (**6**). Only approximate isosbestic behavior was observed due to slight variations in the pathlengths of the sample cells utilized (see Experimental Section). For these preliminary measurements we assume therefore that there are only two principal species in solution, four-coordinate $Cu(LBF_2)$ and five-coordinate $Cu(LBF_2)L'$ (eq 2). Similar measurements with various partial pressures of CO permitted binding constant determinations but, again, no true isosbestic behavior was observed. Table VIII lists the values for the equilibrium constants determined.

Changes in electrochemical redox behavior were also employed to determine equilibrium constants. As shown in Figure 4 and in Table IX the cyclic voltammograms obtained using the Cu(II) complex **5** as starting material depend on both the solvent and on other coordinating ligands in solution. A large excess of 1-MeIm causes a significant negative shift in E^f while excess CO results in a positive shift relative to the cyclic voltammogram obtained for **5** under nitrogen (Figure 4). These shifts are attributable to the formation of Cu(I) and Cu(II) adducts of the ligand added. In Figure 4, curves 1 and 3 have approximately the same wave shape as does curve 2. This suggests that the equilibria between Cu(I), Cu(II), and the added ligands are established rapidly compared to the cyclic voltammetry timescale. In the special case where adducts are formed very rapidly and with only one oxidation state of the metal, the shift in E^f can be correlated simply to the degree of

Table IX. Cyclic Voltammetric Data for $[Cu(LBF_2)ClO_4]_2 \cdot C_4H_8O_2$ (**5**) with Added Ligands[a]

Indicating electrode	Solution atm	L, eq[b]	E_{pc}, V[c]	E_{pa}, V[d]	E^f, V[e]
		In CH_3CN			
Hg	He	None	−0.432	−0.330	−0.381
Pt[d]	N_2	1-MeIm, 5	−0.517	−0.389	−0.453
Pt	N_2	20	−0.548	−0.423	−0.486
Pt	N_2	100	−0.567	−0.437	−0.502
Hg	He	1-MeIm, 100	−0.559	−0.457	−0.508
Hg	CO	CO, satd	−0.274	−0.169	−0.221
		In $(CH_3)_2CO$			
Hg	N_2	None	−0.459	−0.345	−0.402
Pt[d]	He	1-MeIm, 5	−0.561	−0.462	−0.512
Pt	He	20	−0.599	−0.492	−0.546
Pt	He	100	−0.614	−0.502	−0.558
Hg	He	1-MeIm, 100	−0.606	−0.496	−0.551
Hg	CO	CO, satd	−0.298	−0.169	−0.234

[a] Conditions: [Cu] = 2×10^{-3} M; sweep rate = 100 mV/s. [b] L = ligand added, eq = equivalents of L added. [c] Vs. SHE. [d] $E^f \cong E_{pc} + E_{pa}/2$. [e] A Pt indicating electrode was used because with Hg, at approximately +0.035 V, a large reduction wave occurred swamping the Cu(II) + $1e^- \rightarrow$ Cu(I) peak. If the sweep was begun at −0.14 V (CH_3CN) or 0.18 V ($(CH_3)_2CO$) in Hg, the interference was avoided and the cyclical data given were measured. Pt and Hg results agree closely in cases where both were used.

adduct formation.[49] Carbon monoxide as a ligand appears to satisfy these conditions. Addition of CO to the Cu(II) complex **5** causes no observable spectral changes, nor are there any other indications of a Cu(II)-CO adduct. As a first approximation, therefore, the observed shifts in E^f can be totally attributed to formation of the five-coordinate Cu(I) carbonyl $Cu(LBF_2)(CO)$ (**8**). That this is a reasonable assumption is supported by the close approximation between the equilibrium constant obtained (see Experimental and Table VIII) and that found by spectral measurements (Table VIII). Unfortunately, nitrogen bases, including 1-MeIm, bind to both the Cu(I) and the Cu(II) complexes precluding the use of this electrochemical approach to determine equilibrium constants.

The value of K_c for CO ($\sim 4.7 \times 10^4$ M^{-1}) is significantly greater than that for 1-MeIm (16 M^{-1}). Moreover, the shift in E^f for CO is positive, implying stabilization of Cu(I), while that for 1-MeIm is negative, indicative of either stabilization of Cu(II) or destabilization of Cu(I). It can be argued that this may be attributed to the greater π acidity of CO, which serves to drain the 20-electron system of electron density. Such an explanation is not sufficient to account for a number of observations which are discussed below.

Several Cu(I) complexes of polydentate ligands form carbonyl adducts with very similar ν_{CO}'s despite dissimilar structures. In the tetrahedral [hydrotris(pyrazolyl)borato]copper(I) carbonyl and its dimethyl analogue, [hydrotris(3,5-dimethyl-1-pyrazolyl)borato]copper(I) carbonyl, ν_{CO}'s are 2083 and 2066 cm^{-1}, respectively.[38] The presumably four-coordinate (probably distorted square-planar) isoindoline complex **9** has ν_{CO} 2072 cm^{-1}.[39] As reported here, the five-coordinate complex $Cu(LBF_2)(CO)$ (**8**) has ν_{CO} 2068 cm^{-1}. The similarity of ν_{CO} for **8** relative to ν_{CO} in the four-coordinate complexes does not suggest a peculiar bonding situation in the five-coordinate complex which might be expected of a 20-electron species.

The formation of five-coordinate adducts from four-coordinate Cu(I)-macrocyclic ligand complexes is apparently not a general phenomenon. For example, the Cu(I) complex **10**[35] does not change color when exposed to CO, nor is there any shift in E^f as determined by cyclic voltammetry.[50] In contrast, the binuclear mixed-valence Cu(II)Cu(I) carbonyl complex **11** (ν_{CO} 2067 cm^{-1}), which probably contains a five-coordinate Cu(I), has been isolated.[50]

The very formation of five-coordinate Cu(I) is somewhat enigmatic. The $Cu(LBF_2)(CO)$ (**8**) structure (Figure 3) may indicate, however, at least one factor helpful in explaining

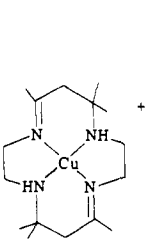

10

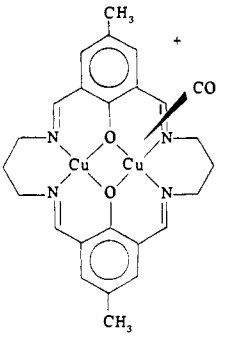

11

five-coordination. The Cu atom is seen to be a full 0.96 Å out of the mean plane of the four coordinating nitrogens of the macrocycle. Such a large displacement of a transition metal atom from a macrocycle is unusual and may be due in part to the large radius of Cu(I). In fact it is not unreasonable to expect that the structure of the four-coordinate species, when determined, will reveal Cu(I) to be significantly displaced from the basal plane of the relatively rigid macrocycle by perhaps as much as 0.4 to 0.5 Å. Poor metal-macrocyclic ligand orbital overlap would undoubtedly result. Though bound to four nitrogen atoms and thus formally an 18-electron system, the Cu(I) atom might be better described as coordinatively unsaturated, sterically if not electronically. In contrast, more flexible ligands, as in **10**, may better accommodate Cu(I), by producing a more tetrahedral environment.

Oxygen Reactivity

Four-coordinate $Cu(LBF_2)$ (**6**) is very oxygen sensitive; royal blue acetone solutions rapidly turn yellow brown. The reaction is irreversible and is dependent on temperature, solvent, and electrolyte concentration. Oxidation products have thus far proven intractable but further work is in progress.

Conclusion

The four-coordinate Cu(I)-macrocyclic ligand complex reacts with certain monodentate ligands to give five-coordinate complexes. The available data are insufficient, but this unusual coordination number for Cu(I) may be partly explained by a rigid ligand environment imposed by the macrocycle. Certainly five-coordination for Cu(I) appears viable and worthy of further study. The complexes described herein are not purported to be accurate mimics of the active sites in any copper proteins.

Table X. Reference Electrode Data for Ferrocene Couple in Water, Acetonitrile, and Acetone

Solvent	$E°$, V	Correction, E', V[c]
Water	+0.400[a]	0.000
Acetonitrile	+0.043[b]	−0.043 + 0.400 = +0.357
Acetone	+0.078[b]	−0.078 + 0.400 = +0.322

[a] Vs. SHE. [b] Vs. $Ag|AgNO_3$ (0.1 M) with 0.1 M tetrabutylammonium perchlorate in acetonitrile. [c] Correction needed to bring measured potentials in acetonitrile, acetone originally vs. $Ag|Ag^+$ (0.1 M) in acetonitrile, to potentials vs. SHE.

Rather they suggest that consideration of Cu(I) active site structures must include the possibility of five-coordination. For example, the binuclear copper site in hemocyanin binds one CO. The carbonyl stretching frequency, $^{51}\nu_{CO}$ 2040–2060 cm^{-1}, indicates CO bound to only one Cu; however, that Cu atom could conceivably have as many as five ligands, including CO. Similarly, the resonance Raman spectra of Cu(II) "blue" copper proteins (type I) are interpretable in terms of five-coordination.[52] Since the "blue" copper proteins apparently serve primarily in electron transfer, it seems unlikely that drastic changes occur in the coordination sphere upon reduction of Cu(II) to Cu(I). In any case the present work would be consistent with five-coordination in the reduced, Cu(I), state as well.

Experimental Section

All operations requiring an inert atmosphere were performed in a Vacuum Atmospheres Dri-lab containing either N_2 or He. Electronic absorption spectroscopy (EAS) was performed on a Cary-14 automatic recording spectrometer while infrared spectra were obtained via KBr pellets or in CH_2Cl_2 solution on a Beckman IR-12 spectrometer.

Tetrabutylammonium perchlorate (Southwestern Analytical Chemicals) was dried exhaustively in vacuo before use. Spectroquality acetonitrile and acetone, dried over 4A molecular sieves, were used for cyclic voltammetry. All other solvents were reagent grade.

Electrochemistry. The apparatus used for constant potential electrolysis (CPE) and cyclic voltammetry consisted of Princeton Applied Research's Model 173 potentiostat–galvanostat coupled with Model 179 Digital coulometer, plus a ramp generator of our own design. For display purposes, both a storage oscilloscope and an X–Y recorder were available.

Constant potential electrolyses and cyclic voltammetry were done in a three compartment H-cell. The cell consisted of 25-mL sample and auxiliary compartments separated by a small center compartment, all separated by medium porosity sintered glass frits. In either CH_3CN or $(CH_3)_2CO$, the supporting electrolyte used was 0.1 M TBAP (tetrabutylammonium perchlorate). The $Ag|Ag^+$ reference electrode consisted of a silver wire immersed in an acetonitrile solution containing $AgNO_3$ (0.1 M) and TBAP (0.1 M), all contained in an 8-mm glass tube fitted on the bottom with a fine porosity sintered glass frit. To provide a more general reference, ferrocene's Fe(II)|Fe(III) couple[53] was examined in CH_3CN and $(CH_3)_2CO$. Table X gives measured data and the corrections which were used throughout this paper to adjust the potentials measured against $Ag|Ag^+$ to potentials vs. SHE.

Formal reduction potentials, E^f, were measured by cyclic voltammetry using the formula $E^f = (E_{p_a} + E_{p_c})/2$. The potentials so determined are approximate in that the systems examined did not display strict reversibility, nor were corrections made for diffusion coefficients.

Determination of Binding Constants. Equation 2 gives the equilibrium expression for the reaction of $Cu(LBF_2)$ (**6**) with ligands, L′. As a first approximation to the equilibrium constant for the formation of five-coordinate species, the equilibrium concentration constant is defined:

$$K_c = [Cu(LBF_2)L']/[Cu(LBF_2)][L'] \quad (3)$$

The equilibrium concentrations of the Cu complexes were determined by use of the Beer's law dependence of the $Cu(LBF_2)$ 677-nm band. It was assumed that $Cu(LBF_2)L'$ did not absorb appreciably at 677 nm. Therefore, when $Cu(LBF_2)$ reacted with L′, ΔA ($A_{initial} - A_{equilibrium}$) was taken as a measure of $Cu(LBF_2)L'$ formed.

With L′ = 1-MeIm, the cells used had measured pathlengths of about 1 mm. The short pathlength permitted relatively high concentrations of $Cu(LBF_2)$ to be used, thus minimizing decomposition due to residual dissolved oxygen. Preparation of solutions of $Cu(LBF_2)$ ($[Cu(LBF_2)]_{initial} \cong 8 \times 10^{-4}$ M) and addition of 1-MeIm ($[1\text{-MeIm}]_{initial} = 2 \times 10^{-3}$ to 1 M) was effected in the inert atmosphere chamber. The cells were closed with greased, glass stoppers and taped. Spectra were recorded to determine ΔA (677 nm). Measurements were made at 30 ± 2 °C. Only approximate isosbestic behavior was observed, most probably owing to the slight variation in pathlengths of the several cells employed (e.g., see Figure 3). If a 1:1 stoichiometry for adduct formation is assumed (eq 2), the constant K_c is found to be 16 ± 3 M^{-1}.

For CO measurements, the cells used each had approximately 1-mm pathlengths, a 10-mL side-arm reservoir, a Teflon high-vacuum stopper, and a standard taper joint for attachment to a vacuum line. The $Cu(LBF_2)$ ($[Cu(LBF_2)]_{initial} \cong 1.6 \times 10^{-3}$ M) solutions were prepared in the inert atmosphere chamber and closed to the atmosphere. The solutions were then degassed by the freeze–pump–thaw technique (3 cycles) on the vacuum line. The spectra were measured before addition of CO.

The $Cu(LBF_2)$ solution was opened to a system with a mercury manometer and an acetone reservoir. The acetone vapor pressure was measured when the system had equilibrated. Addition of CO (10–80 mmHg) was monitored by use of the manometer. The $Cu(LBF_2)$ solution was stirred under CO for 20 min and the pressure and temperature were then recorded. The spectra were recorded in order to find ΔA (677 nm). A plot of $[Cu(LBF_2)(CO)]/[Cu(LBF_2)]$ vs. P(CO) was extrapolated to give $P_{1/2}(CO) = 1.5$ mm when the $[Cu(LBF_2)(CO)] = [Cu(LBF_2)]$. The equilibrium (pressure) constant, K_p, was calculated as 500 ± 15 atm^{-1}.

Conversion of K_p to K_c for the purpose of comparison to K_c (1-MeIm) utilized data for CO solubility in acetone. Use of a value of 0.2358 mL of CO per mL of acetone at 20 °C[54] and of Henry's law allowed conversion of $P(CO)$ to [CO]. Calculation of K_c resulted in a value of $4.7 \pm 0.2 \times 10^4$ M^{-1}.

The CO binding constant $K_c(CO)$ was also estimated via the shift in E^f. Cyclic voltammograms of the Cu(II) complex **5** (acetone/Hg) under 1 atm of CO showed a shift of E^f of 0.168 V vs. that found under N_2 (Table IX). Such shifts can be related to the binding of ligand to metal in both the oxidized and the reduced state.[49] A simplified relationship can be derived for the case in which ligand binds, effectively, to only one oxidation state, e.g., eq 4.

$$[Cu(LBF_2)]^+ + CO + e^- \rightleftharpoons [Cu(LBF_2)(CO)] \quad (4)$$

In this equation

$$E°_{(CO)} = E° + (RT/F) \ln (1 + K_c[CO])$$

$E°$ and $E°_{(CO)}$ are the standard potentials for the reduction in the absence and presence of CO, respectively. The equilibrium constant K_c was calculated using the appropriate formal potentials E^f in place of the standard potentials $E°$.

X-Ray Data Collection. Crystals of the carbonyl adduct were grown by quick evaporation of an acetone solution under carbon monoxide. Weissenberg photographs revealed orthorhombic symmetry and systematic absences: $h = 2n + 1$, $hk0$ data; $k = 2n + 1$, $0kl$ data; $l = 2n + 1$, $h0l$ data. These extinctions are consistent only with the space group *Pbca*.

A multifaceted crystal of dimensions 0.15 mm × 0.15 mm × 0.30 mm was positioned on a Datex-automated General Electric quarter-circle diffractometer with the [001] direction nearly coincident with the ϕ axis of the diffractometer. The lattice parameters (Table I) were determined by a least-squares fit of 14 manually centered reflections. Data were collected out to $2\theta_{max} = 130°$ above which only a small number of the reflections had measurable intensity. The scan widths were varied linearly from 1.80° at $2\theta = 3°$ to 3.50° at $2\theta = 130°$. The scan speed was 2° min^{-1}. Intensities of 2738 reflections were measured by the moving-crystal, moving-counter techniques using a takeoff angle of 3°. The total background time was 40 s. Three reflections measured every 25 reflections served to monitor crystal and instrumental stability. No significant falloff in the intensities of these reflections was observed.

The measured intensities were reduced to structure factor amplitudes by applying Lorentz and polarization corrections. The standard deviations in the intensities were calculated from the formula: $\sigma^2(I) = S + (B1 + B2)T^2 + (dS)^2$, where S, $B1$, and $B2$ are the scan counts and two background counts, T is a factor which corrects for the difference in time spent on the scan and background counts, and d is the Peterson-Levy[55] factor taken to be 0.02. For the purpose of an absorption correction, the shape of the crystal was approximated by a rectangular prism.

Solution and Refinement of the Structure. The position of the copper atom was determined from a three-dimensional Patterson map. Difference-Fourier syntheses revealed the positions of all the other nonhydrogen atoms. Full-matrix isotropic refinement[56] with data out to 100° in 2θ lowered the R factor to 10%. At this point hydrogen atoms were included. After additional least-squares, a systematically negative disparity between the observed and calculated structure factors was noted. A secondary extinction parameter was included in the refinement as a correction.[61] Least-squares refinement was continued to convergence with two matrices; one matrix contained all nonhydrogen atom coordinates and anisotropic temperature factors, the other contained coordinates of the hydrogen atoms. Isotropic thermal parameters of the hydrogen atoms were fixed at the value of the carbon atom to which they were bonded plus 1.0 Å^2. The R factor[62] at the end of the refinement was 5.5% for 2511 data ($F_o^2 > 0$). No observations other than systematically absent reflections were omitted from the refinement. The goodness of fit was 1.39. A final difference-Fourier synthesis showed no residual electron density greater than 0.34 e Å^{-3}.

Final positional parameters are given in Table VI. Table VII lists the anisotropic thermal parameters.

Preparation of Complexes. 3,3′-(Trimethylenedinitrilo)bis(2-butanone oxime), H_2L (1). 1,3-Propanediamine (37.06 g, 0.5 mol) and 2,3-butanedione monoxime (101.0 g, 1.0 mol) were mixed together in hot ethanol to give a yellow solution approximately 250 mL volume. The solution was allowed to cool to ambient temperature. The resulting white precipitate was isolated immediately by vacuum filtration, washed well with diethyl ether, and dried in air. The ligand was used without further purification.

[3,3′-(Trimethylenedinitrilo)bis(2-butanone oximato)]copper(II) Perchlorate Monohydrate, $(Cu(LH)ClO_4 \cdot H_2O$ (2). A hot acetone solution (20 mL) of $Cu(ClO_4)_2 \cdot xH_2O$ (dried in vacuo at 25 °C, 3.7 g, 10 mmol) was added to a hot acetone solution of the ligand, H_2L, **1** (4.8 g, 20 mmol, in 20 mL), giving a deep red solution. As the solution cooled, a dark red-brown crystalline product precipitated. The solid was isolated by vacuum filtration, washed with diethyl ether, and dried in air. Anal. Calcd for $C_{11}H_{21}ClCuN_4O_7$: C, 31.45; H, 5.00; N, 13.3; Cu, 15.1. Found: C, 31.55; H, 4.75; N, 13.3; Cu, 16.0.

Millimolar solutions of this compound were examined by cyclic voltammetry. A quasireversible wave, complicated by a copper stripping wave, yielded an $E^f \cong 0.56$ V. Constant potential electrolysis at −0.8 V caused the purple solution to become blue with a small amount of copper being plated out on the platinum working electrode. The n values were slightly greater than 1.

Bis[difluoro-3,3′-(trimethylenedinitrilo)bis(2-butanone oximato)boratecopper(II) Perchlorate] Monodioxane, $(Cu(LBF_2)ClO_4)_2 \cdot C_4H_8O_2$ (5). Boron trifluoride etherate, $BF_3 \cdot Et_2O$ (6 mL, 50 mmol), was added slowly, with stirring, to a mixture of $Cu(LH)ClO_4 \cdot H_2O$ (**2**) (7.0 g, 17 mmol) in warm dioxane (150 mL, 70 °C). The mixture was heated, with stirring, at a boil for 1 h. The red-violet mixture was cooled slowly to ambient temperature. Dark red-violet solid was isolated by vacuum filtration, washed well with dioxane and diethyl ether, and dried in air. The product was dissolved in a minimum amount of boiling acetone (150 mL). The hot solution was filtered and treated with 5 mL of dioxane. Crystalline product, obtained upon cooling, was isolated and treated as before. A yield of 5.3 g (64%) was obtained. Anal. Calcd for $C_{26}H_{44}B_2Cl_2Cu_2F_4N_8O_{14}$: C, 31.6; H, 4.45; N, 11.35; Cu, 12.85. Found: C, 31.9; H, 4.5; N, 11.25; Cu, 12.6.

[Difluoro-3,3′-(trimethylenedinitrilo)bis(2-butanone oximato)borate]copper(I), $Cu(LBF_2)$ (6). This copper(I) complex was prepared by constant potential electrolysis in a He atmosphere chamber. A simple H-cell was employed with 0.1 M TBAP in acetone in all three chambers. The Cu(II) complex $[Cu(LBF_2)ClO_4]_2 \cdot C_4H_8O_2$, (**5**) (0.8 g, 15 mmol) was dissolved in the cathodic compartment which also contained a magnetic stir bar and a platinum gauze electrode. A self-contained $Ag|Ag^+$ reference electrode was placed in the middle chamber while a platinum wire was employed in the anodic chamber. Constant potential electrolysis was carried out at −1.0 V vs. $Ag|Ag^+$ (−0.678 V vs. SHE; see Table X) until the current was 1% of the initial value. During electrolysis, red $Cu(LBF_2)$ (**6**) crystallized from solution. The product was isolated by vacuum filtration, washed with ethanol, and dried under He. Anal. Calcd for $C_{11}H_{18}BCuF_2N_4O_2$: C, 37.65; H, 5.15; N, 16.0; Cu, 18.1. Found: C, 37.8; H, 5.1; N, 16.1; Cu, 18.2; ϵ(acetone, 25 °C, 677 nm) = 1.03 ± 0.02 × 10^4 M^{-1} cm^{-1}. A magnetic susceptibility measurement by the Faraday method showed the compound to be diamagnetic at 25 °C.

Carbonyl[difluoro-3,3′-(trimethylenedinitrilo)bis(2-butanone oximato)borate]copper(I), $Cu(LBF_2)(CO)$ (8). A blue solution of $Cu(LBF_2)$ (**6**) (0.35 g, 10 mmol) in acetone (25 mL) under N_2 was treated with CO (1 atm) yielding a greenish-yellow solution with some green solid. The green solid was removed by filtration and the resulting filtrate was treated with slow additions of heptane. The resulting orange crystalline product was isolated by filtration and dried under a stream of CO. Anal. Calcd for $C_{12}H_{18}BCuF_2N_4O_3$: C, 38.05; H, 4.75; N, 14.8; Cu, 16.8. Found: C, 38.1; H, 4.9; N, 14.7; Cu, 17.1.

[Difluoro-3,3′-(trimethylenedinitrilo)bis(2-butanone oximato)borate](1-methylimidazole)copper(I), $Cu(LBF_2)$(1-MeIm) (7). 1-Methylimidazole (0.1 g, 1.2 mmol) was added under nitrogen to a blue solution of $Cu(LBF_2)$ (**6**) (0.1 g, 0.2 mmol) in acetone (15 mL). A dark emerald-green solution resulted. Aliquots of heptane (5 mL) were added every 10 min until 30 mL total had been added. After 2 h, red crystalline product (red even when ground to a powder) was isolated by vacuum filtration, washed with 1:1 acetone:heptane, and dried under N_2. Anal. Calcd for $C_{15}H_{24}BCuF_2N_6O_2$: C, 41.6; H, 5.55; N, 19.4; Cu, 14.7. Found: C, 42.0; H, 5.55; N, 19.6; Cu, 14.4.

Note Added in Proof. Crystallographic analysis shows complex **6** to contain essentially square-planar Cu(I) with the four-coordinated nitrogen atoms distorted slightly toward tetrahedrality.[63]

Acknowledgment. We appreciate the assistance of F. Anson, G. Mauk, J. Fujitaki, and J. Koval. This work was supported by the National Institutes of Health and the National Science Foundation.

Supplementary Material Available: Listing of structure factor amplitudes (11 pp). Ordering information is given on current masthead page.

References and Notes

(1) J. Peisach, P. Aisen, and W. E. Blumberg, "The Biochemistry of Copper", Academic Press, New York, N.Y., 1966.
(2) W. H. Vanneste and A. Zuberbühler in "Molecular Mechanisms of Oxygen Activation," O. Hayaishi, Ed., Academic Press, New York, N.Y., 1974, p 371
(3) R. Malkin in "Inorganic Biochemistry", G. L. Eichhorn, Ed., Elsevier, New York, N.Y., 1973, p 689.
(4) In certain copper-containing proteins the copper appears to serve principally in electron transport with no evidence of Cu–O_2 interaction, e.g., as in cytochrome oxidase.[5] In contrast hemocyanin[6-8] and tyrosinase[9] apparently rely on direct, covalent interaction between Cu(I) and O_2, both forming observable dioxygen adducts. The four-copper protein, laccase, may also rely on covalent interaction between O_2 and a binuclear, type III, Cu site.[10-12]
(5) W. S. Caughey, W. J. Wallace, J. A. Volpe, and S. Yoshikawa, *Enzymes*, **12**, 299 (1975).
(6) K. E. Van Holde and E. F. J. Van Bruggen in "Biological Macromolecules Series", Vol. 5, S. M. Timasheff and G. D. Fasman, Ed., Marcel Dekker, New York, N.Y., 1971.
(7) R. Lontie and R. Witters in ref 3, p 344.
(8) J. Bonaventura, C. Bonaventura, and B. Sullivan, *J. Exp. Zool.*, **194**, 155 (1975).
(9) (a) R. L. Jolley, Jr., L. H. Evans, and H. S. Mason, *Biochem. Biophys. Res. Commun.*, **46**, 878 (1972); (b) R. L. Jolley, Jr., L. H. Evans, N. Makino, and H. S. Mason, *J. Biol. Chem.*, **249**, 335 (1974).
(10) R. Aasa, R. Branden, J. Deinum, B. G. Malmstrom, B. Reinhammer, and T. Vanngard, *FEBS Lett.*, **61**, 115 (1976).
(11) R. Branden and J. Deinum, *FEBS Lett.*, **73**, 144 (1977).
(12) O. Farver, M. Goldberg, D. Lancet, and I. Pecht, *Biochem. Biophys. Res. Commun.*, **73**, 494 (1976).
(13) B. Reinhammer, *Biochim. Biophys. Acta*, **205**, 35 (1970).
(14) K. Lerch, *FEBS Lett.*, **69**, 157 (1976).
(15) A. J. M. Schoot Uiterkamp, H. VanDerDeen, H. C. J. Berendsen, and J. F. Boas, *Biochim. Biophys. Acta*, **372**, 407 (1974).
(16) A. J. M. Schoot Uiterkamp, *FEBS Lett.*, **20**, 93 (1972).
(17) A. J. M. Schoot Uiterkamp and H. S. Mason, *Proc. Natl. Acad. Sci. U.S.A.*, **70**, 993 (1973).
(18) N. Makino, P. McMahill, H. S. Mason, and T. H. Moss, *J. Biol. Chem.*, **249**, 6662 (1974).

(19) E. I. Solomon, D. M. Dooley, R.-H. Wang, H. B. Gray, M. Cerdonio, F. Mogno, and G. L. Romani, *J. Am. Chem. Soc.*, **98**, 1029 (1976).
(20) T. H. Moss, D. C. Gould, A. Ehrenberg, J. S. Loehr, and H. S. Mason, *Biochemistry*, **12**, 2444 (1973).
(21) Y. Engelborghs, S. H. DeBruin, and R. Lontie, *Biophys. Chem.*, **4**, 343 (1976).
(22) B. Salvato, A. Ghiretti-Magaldi, and F. Ghiretti, *Biochemistry*, **13**, 4778 (1974).
(23) J. S. Loehr, T. B. Freedman, and T. M. Loehr, *Biochem. Biophys. Res. Commun.*, **56**, 510 (1974).
(24) T. B. Freedman, J. S. Loehr, and T. M. Loehr, *J. Am. Chem. Soc.*, **98**, 2809 (1976).
(25) R. H. Jardine, *Adv. Inorg. Biochem.*, **17**, 115 (1975).
(26) There are several reports of reversible oxygenation in solution or complexes whose stoichiometry implies possible dioxygen complexation, but these are poorly characterized. See (a) T. Graf and S. Fallab, *Experientia*, **20**, 46 (1964); (b) E. Ochiai, *Inorg. Nucl. Chem. Lett.*, **9**, 987 (1973); (c) C. E. Kramer, G. Davies, R. B. Davis, and R. W. Slaven, *J. Chem. Soc., Chem. Commun.*, 606 (1975); (d) C. S. Arcus, J. L. Wilkinson, C. Meali, T. J. Marks, and J. A. Ibers, *J. Am. Chem. Soc.*, **96**, 7564 ([974(/
(27) R. W. Erskine and B. O. Field in "Structure and Bonding", Vol. 28, Springer-Verlag, New York, N.Y., 1976, p 1.
(28) A. V. Savitskii and V. I. Nelyubin, *Russ. Chem. Rev.*, **44**, 110 (1975).
(29) J. S. Valentine, *Chem. Rev.*, **73**, 235 (1973).
(30) V. J. Choy and C. J. O'Connor, *Coord. Chem. Rev.*, 9, 145 (1972–73).
(31) R. R. Gagné, *J. Am. Chem. Soc.*, **98**, 6709 (1976).
(32) For an excellent review see: W. E. Hatfield and R. Whyman, *Trans. Metal Chem.*, **5**, 47 (1969).
(33) F. A. Cotton and G. Wilkinson In "Advanced Inorganic Chemistry", 3rd ed, Interscience, New York, N.Y., 1972, p 905.
(34) G. S. Patterson and R. H. Holm, *Bioinorg. Chem.*, **4**, 257 (1975).
(35) D. C. Olson and J. Vasilevskis, *Inorg. Chem.*, **10**, 463 (1971).
(36) There are notable exceptions; see ref 37–39.
(37) M. I. Bruce and A. P. P. Ostazewski, *J. Chem. Soc., Dalton Trans.*, 2433 (1973).
(38) C. Meali, C. S. Arcus, J. L. Wilkinson, T. J. Marks, and J. A. Ibers, *J. Am. Chem. Soc.*, **98**, 711 (1976).
(39) R. R. Gagne, L. Speltz, and R. Gall, manuscript in preparation.
(40) E. Uhlig and M. Friedrich, *Z. Anorg. Allg. Chem.*, **343**, 299 (1966).
(41) R. M. Countryman, W. T. Robinson, and E. Sinn, *Inorg. Chem.*, **13**, 2013 (1974).
(42) Another quasireversible wave, which is comparable in size to the wave depicted in Figure 1, appears at far more negative potentials, $E^f \cong -1.2$ V. This process may be attributable to reduction of the ligand.
(43) F. Bigoli, A. Brarbanti, A. Tiripicchio, and M. Tiripicchio Camellini, *Chem. Commun.*, 120 (1970), for example.
(44) M. R. Churchill, B. G. DeBoer, F. J. Rotella, O. M. Abu Salah, and M. I. Bruce, *Inorg. Chem.*, **14**, 2051 (1975).
(45) (a) J. P. Collman, P. A. Christian, S. Current, P. Denisevich, T. R. Halbert, E. R. Schmittou, and K. O. Hodgson, *Inorg. Chem.*, **15**, 223 (1976); (b) S. Bruckner, M. Calligaris, G. Nardin, and L. Randaccio, *Inorg. Chim. Acta*, **3**, 278 (1969).
(46) I. B. Liss and E. O. Schlemper, *Inorg. Chem.*, **14**, 3035 (1975).
(47) (a) J. P. Collman and M. R. MacLaury, *J. Am. Chem. Soc.*, **96**, 3019 (1974); (b) J. P. Collman, D. W. Murphy, and G. Dolcetti, *Ibid.*, **95**, 2687 (1973).
(48) The standard deviation of the mean is calculated by the formula $[\sum^{N}_{i=i}(X_i - X)^2/N - 1)]^{1/2}$.
(49) J. Heyrovski and J. Kuta, "Principles of Polarography", Academic Press, New York, N.Y., 1966, p 157.
(50) R. R. Gagné, C. Koval, T. Smith, and M. Cimolino, manuscript in preparation.
(51) (a) L. Y. Fager and J. O. Alben, *Biochemistry*, **11**, 4786 (1972); (b) J. O. Alben, L. Yen, and N. J. Farrier, *J. Am. Chem. Soc.*, **92**, 4475 (1970).
(52) V. Miskowski, S.-P. W. Wang, T. G. Spiro, E. Shapiro, and T. H. Moss, *Biochemistry*, **14**, 1244 (1975).
(53) D. Baner and M. Breant, in "Electroanalytical Chemistry", Vol. VIII, A. J. Bard, Ed., Marcel Dekker, New York, N.Y., 1975, p 306.
(54) J. Horiuti, *Sci. Pap. Inst. Phys. Chem. Res. (Jpn.)*, **17**, 125 (1931).
(55) S. W. Peterson and H. A. Levy, *Acta Crystallogr.*, **10**, 70 (1957).
(56) Except for C. K. Johnson's ORTEP program, the computer programs used were from the CRYM system of crystallographic computer programs. The function minimized in the least-squares refinement was $\Sigma w(F_o^2 - F_c^2)^2$ where F_o and F_c are the observed and calculated structure factors and the weights, w, are $1/\sigma^2(F_o^2)$. Neutral atom scattering factors for Cu were taken from the compilation of Cromer and Waber;[57] those for the other nonhydrogen atoms were from ref 58. Hydrogen atom scattering factors are those of Stewart et al.[59] The real component of the anomalous dispersion correction[60] was included for Cu.
(57) D. T. Cromer and J. T. Waber, *Acta Crystallogr.*, **18**, 104 (1965).
(58) "International Tables for X-Ray Crystallography", Vol. III, Kynoch Press, Birmingham, England, 1962.
(59) R. F. Stewart, E. R. Davidson, and W. T. Simpson, *J. Chem. Phys.*, **42**, 3175 (1965).
(60) D. T. Cromer, *Acta Crystallogr.*, **18**, 17 (1965).
(61) The form of the correction for secondary extinction is $F_c = F_o(1 + cI_c)$. The value from the refinement is 2.00 (9) $\times 10^{-6}$ e^{-2}.
(62) The R index is $\Sigma|F_o - F_c|/\Sigma|F_o|$. The goodness of fit is $\Sigma w(F_o^2 - F_c^2)^2/(n - p)$, where n is the number of observations and p is the number of parameters.
(63) R. R. Gagné, J. L. Allison, and G. Lisensky, manuscript in preparation.

Aggregation in High-Spin Ferric Complexes of Tetraarylporphyrins. Structure Determination Using Intermolecular Electron–Nuclear Dipolar Relaxation

Richard V. Snyder and Gerd N. La Mar*

Contribution from the Department of Chemistry, University of California, Davis, California 95616. *Received April 25, 1977*

Abstract: The ^{1}H NMR spectra of the high-spin ferric halide complexes of tetra-*p*-tolylporphyrins are shown to exhibit concentration-dependent line width and chemical shifts indicative of significant aggregation in solution. The degree of aggregation is shown to increase with solvent dielectric constant in chloroform-*d*, methylene chloride-d_2, and toluene-d_8, and with halide ion in a given solvent in the order I > Br > Cl. The intermolecular paramagnetic dipolar relaxation is shown to be highly stereospecific, permitting a qualitative description of the structure of the proposed dominant dimer at intermediate concentrations. The structure consists of pairs of overlapping pyrroles in contact on the side of the porphyrin opposite to the out-of-plane iron. At higher concentrations, additional aggregated species exist. The results indicate that intermolecular paramagnetic dipolar relaxation may serve as a very useful tool for elucidating the solution structure of porphyrin aggregates.

One of the characteristic properties of porphyrins and metalloporphyrins is the tendency to dimerize or aggregate in solution. Two general types of aggregates have been characterized,[1,2] those involving the formation of a covalent bond linking the porphyrins within an aggregate via either a bridging ligand, metal–metal bond, or intermolecular coordination of basic side chains, and those based on van der Waals interactions involving primarily the porphyrin π systems. The covalently linked aggregates have been generally easier to characterize and much more work has been devoted to their study than to the van der Waals aggregates.[1,2] Particularly little is known about the factors influencing the noncovalent porphyrin interactions in nonaqueous systems. It is precisely these van der Waals π–π interactions in a hydrophobic environment between the porphyrin π cloud and aromatic amino acid side chains which are important in all known hemoproteins.[3]

Although the tendency for natural porphyrin derivatives to aggregate in a noncovalent manner is well recognized, it has been generally accepted[1] that the more or less perpendicular orientation of the phenyl groups in the synthetic *meso*-